

# Selective IL-1 $\alpha$ exposure to the fetal gut, lung, and chorioamnion/skin causes intestinal inflammatory and developmental changes in fetal sheep

Maria Nikiforou<sup>1,2</sup>, Matthew W Kemp<sup>3</sup>, Rick H van Gorp<sup>2,4</sup>, Masatoshi Saito<sup>3,5</sup>, John P Newnham<sup>3</sup>, Niki L Reynaert<sup>6</sup>, Leon EW Janssen<sup>1,2</sup>, Alan H Jobe<sup>3,7</sup>, Suhas G Kallapur<sup>3,7</sup>, Boris W Kramer<sup>1,2,4</sup> and Tim GAM Wolfs<sup>2,4</sup>

Chorioamnionitis, caused by intra-amniotic exposure to bacteria and their toxic components, is associated with fetal gut inflammation and mucosal injury. In a translational ovine model, we have shown that these adverse intestinal outcomes to chorioamnionitis were the combined result of local gut and pulmonary-driven systemic immune responses. Chorioamnionitis-induced gut inflammation and injury was largely prevented by inhibiting interleukin-1 (IL-1) signaling. Therefore, we investigated whether local (gut-derived) IL-1 $\alpha$  signaling or systemic IL-1 $\alpha$ -driven immune responses (lung or chorioamnion/skin-derived) were sufficient for intestinal inflammation and mucosal injury in the course of chorioamnionitis. Fetal surgery was performed in sheep to isolate the lung, gastrointestinal tract, and chorioamnion/skin, and IL-1 $\alpha$  or saline was given into the trachea, stomach, or amniotic cavity 1 or 6 days before preterm delivery. Selective IL-1 $\alpha$  exposure to the lung, gut, or chorioamnion/skin increased the CD3+ cell numbers in the fetal gut. Direct IL-1 $\alpha$  exposure to the gut impaired intestinal zonula occludens protein-1 expression, induced villus atrophy, changed the expression pattern of intestinal fatty acid-binding protein along the villus, and increased the CD68, IL-1, and TNF- $\alpha$  mRNA levels in the fetal ileum. With lung or chorioamnion/skin exposure to IL-1 $\alpha$ , intestinal inflammation was associated with increased numbers of blood leukocytes without induction of intestinal injury or immaturity. We concluded that local IL-1 $\alpha$  signaling was required for intestinal inflammation, disturbed gut maturation, and mucosal injury in the context of chorioamnionitis.

*Laboratory Investigation* (2016) 96, 69–80; doi:10.1038/labinvest.2015.127; published online 26 October 2015

Intrauterine infection is the most frequent cause of preterm birth<sup>1</sup> before 28 weeks of gestation.<sup>2</sup> Chorioamnionitis, which is commonly caused by intrauterine bacterial infection, is defined as an inflammation of the fetal membranes, amniotic fluid and placenta.<sup>3–5</sup> Bacterial infection of the amniotic cavity results in direct exposure of the lung (by fetal breathing), gastrointestinal tract (by swallowing), skin, and chorioamnion to bacteria and their inflammatory components in the contaminated amniotic fluid. The fetal inflammatory response to chorioamnionitis is associated with multiorgan dysfunction,<sup>6,7</sup> which increase the incidence of periventricular leukomalacia,<sup>8</sup> bronchopulmonary dysplasia,<sup>9</sup> and necrotizing enterocolitis.<sup>10,11</sup>

We have used a translational ovine model of chorioamnionitis to investigate the impact of intrauterine inflammation on fetal organs. Using this model, we have shown that intra-amniotic (IA) delivery of *Escherichia coli* lipopolysaccharide (LPS) resulted in an acute inflammatory response in the chorioamnion and increased the influx of inflammatory cells in the respiratory tract within 5 h.<sup>12,13</sup> These immune alterations were rapidly followed by systemic inflammation at the same time point and fetal skin inflammation 12 h after LPS exposure.<sup>13,14</sup> The first signs of intestinal inflammation were detected 2 days after IA delivery of LPS, and this inflammatory response resulted from direct LPS exposure to the gut and pulmonary-induced systemic inflammation.<sup>15</sup>

<sup>1</sup>School for Mental Health and Neuroscience, Maastricht University, Maastricht, The Netherlands; <sup>2</sup>Department of Pediatrics, Maastricht University Medical Center, Maastricht, The Netherlands; <sup>3</sup>School of Women's and Infants' Health, The University of Western Australia, Perth, WA, Australia; <sup>4</sup>School of Oncology and Developmental Biology, Maastricht University, Maastricht, The Netherlands; <sup>5</sup>Division of Perinatal Medicine, Tohoku University Hospital, Sendai, Japan; <sup>6</sup>School for Nutrition and Translational Research in Metabolism, Department of Respiratory Medicine, Maastricht University Medical Center, Maastricht, The Netherlands and <sup>7</sup>Division of Pulmonary Biology, Cincinnati Children's Hospital Medical Centre, University of Cincinnati School of Medicine, Cincinnati, OH, USA  
Correspondence: Dr TGM Wolfs, PhD, Department of Pediatrics, Maastricht University Medical Center, Universiteitssingel 50, Maastricht 6200 MD, The Netherlands.  
E-mail: tim.wolfs@maastrichtuniversity.nl

Received 21 April 2015; revised 31 July 2015; accepted 17 August 2015

**Table 1 Summary of experimental groups with fetal compartments exposed to IL-1 $\alpha$  or saline**

Procedure	Site of exposure	1 Day exposure		6 Days exposure	
		<i>n</i>	Abbreviation	<i>n</i>	Abbreviation
Lung isolation tracheal infusion of IL-1 $\alpha$	Lung	7	1d lung IL-1 $\alpha$	8	6d lung IL-1 $\alpha$
Gut isolation stomach infusion of IL-1 $\alpha$	Gut	5	1d gut IL-1 $\alpha$	6	6d gut IL-1 $\alpha$
Snout occlusion IA infusion of IL-1 $\alpha$	Amniotic cavity, skin	5	1d Ocln IL-1 $\alpha$	4	6d Ocln IL-1 $\alpha$
Combined controls <sup>a</sup> infusion of saline	Lung or gut or chorioamnion/skin <sup>a</sup>	4	Control	5	Control

d, day(s); IA, intra-amniotic; IL, interleukin; *n*, number of animals; Ocln, snout occlusion.

<sup>a</sup>Combined control group of all saline-treated animals.

Importantly, inhibition of IL-1 signaling with an IL-1 receptor antagonist in our chorioamnionitis model largely prevented fetal organ inflammation and its negative sequelae.<sup>16,17</sup> IL-1 signaling is central to antenatal inflammation in multiple animal models,<sup>18–20</sup> and IA IL-1 $\alpha$  administration in fetal sheep caused inflammation in the chorioamnion with injury to the respiratory and gastrointestinal tract.<sup>21–23</sup> However, it remains unstudied whether local (i.e. gut-derived) IL-1 $\alpha$  signaling or systemic IL-1 $\alpha$ -driven immune activation (i.e. lung- or chorioamnion/skin-derived) is causally involved in intestinal inflammation and mucosal injury from chorioamnionitis.

To answer this question, we surgically isolated the lung, gastrointestinal tract, and chorioamnion/skin in fetal sheep for selective IL-1 $\alpha$  exposure 1 or 6 days before preterm delivery. We evaluated the systemic and intestinal immune responses of IL-1 $\alpha$  exposure to the different isolated fetal compartments.

## MATERIALS AND METHODS

### Animals

All experiments were approved by the Animal Ethics Committee of the University of Western Australia (Perth, WA, Australia) and the Children's Hospital Medical Center (Cincinnati, OH, USA).

### Experimental Procedures and Design

Experimental procedures were performed as described previously.<sup>15</sup> Fetal sheep were randomized to experimental groups as defined in Table 1. Fetal surgery was performed at 116 or 121 days of gestational age (GA) (term ~ 150 days). Fetuses received either IL-1 $\alpha$  (Protein Express, Cincinnati, OH, USA) or saline (control) at 118 or 123 days GA via a 24 h osmotic pump. We used the following doses: 10  $\mu$ g of IL-1 $\alpha$  for intratracheal infusion, 50  $\mu$ g of IL-1 $\alpha$  for gastrointestinal infusion, and 100  $\mu$ g of IL-1 $\alpha$  for IA infusion. A dose of 100  $\mu$ g IL-1 $\alpha$  into the amniotic cavity induces chorioamnionitis and inflammation in the lung and gut with concomitant developmental changes.<sup>21,22</sup> Intratracheal infusion of IL-1 $\alpha$  (10  $\mu$ g) causes pulmonary inflammation and maturation.<sup>24</sup> As

the swallowing volume rate of the fetus is ~ 50% of the total amniotic volume over 24 h,<sup>25</sup> a dose of 50  $\mu$ g of IL-1 $\alpha$  was infused to the GI tract. Fetal sheep were surgically delivered at 124 days of gestation and were killed with an intravenous bolus of pentobarbitone (100 mg/kg) 1 or 6 days after IL-1 $\alpha$  or saline infusion.

Isolation of the fetal organs was performed as described previously.<sup>15</sup> Briefly, fetal lung isolation: a catheter was connected to an osmotic pump to administer IL-1 $\alpha$  or saline for controls. The trachea and esophagus were ligated to prevent contact with the amniotic fluid; isolation of the fetal gastrointestinal tract: a catheter was placed via the esophagus into the stomach and an osmotic pump was used to administer IL-1 $\alpha$  or saline for controls. The esophagus was ligated to avoid IL-1 $\alpha$  reaching the amniotic fluid; isolation of the fetal snout: selective exposure of IL-1 $\alpha$  in the skin and chorioamnion was achieved by occlusion of the snout with a surgical glove. An osmotic pump was sutured to the fetal skin and delivered IL-1 $\alpha$  or saline for controls.

### Cell Count Measurement in Cord Blood

Differential cell counts in the cord blood were performed by Coulter counter (VetPath Laboratory Services, Ascot, WA, Australia).

### Antibodies

The following antibodies were used: rabbit antibody against human cluster of differentiation 3 (CD3; 1:1000) and myeloperoxidase (MPO; 1:500) both from Dako (Glostrup, Denmark); intestinal fatty acid-binding protein (I-FABP; 1:3000) from Hycultbiotech (Uden, The Netherlands); rabbit antibody against mouse zonula occludens protein-1 (ZO-1; 1:100) from Invitrogen (San Francisco, CA, USA); monoclonal mouse antibody against human forkhead box P3 (FoxP3; 1:250) from Bioscience (San Diego, CA, USA); mouse anti-human Ki-67 (1:100) from Dako (Glostrup, Denmark) and rabbit anti-human caspase-3 (1:1000) from Cell Signaling Technology (Danvers, MA, USA). As secondary antibodies, Texas Red-conjugated goat anti-rabbit (1:100) from Southern Biotechnology (Birmingham, AL, USA); biotin-conjugated

**Table 2 Primers used for qPCR**

Primer	Fw sequence (5'–3')	Rv sequence (5'–3')
ovRPS15	CGAGATGGTGGGCAGCAT	GCTTGATTCCACCTGGTTGA
TNF- $\alpha$	GCCGGAATACCTGGACTATGC	CAGGGCGATGATCCCAAAGTAG
IL-6	ACATCGTCGACAAAATCTCTGCAA	GCCAGTGTCTCCTTGCTGTTT
IL-17	TGTGAGGGTCAACCTGAACAT	TGATAATCGGTGGGCCTTCTG
IL-1	AGAATGAGCTGTTATTTGAGGTTGATG	GTGAGAAATCTGCAGCTGGATGT
IFN- $\gamma$	TCAAGCAAGACATGTTTCAGAAGTCT	CCGGAAATTTGAATCAGCCTTTTGAA
CD68	AGGCAGTGCAGTGGACATTC	CAAGGTGTAAGCTGGTGAAC
IL-4	TGCCTGTAGCAGACGTCTTTG	GCCCTGCAGAAGGTTTCT
IL-10	CATGGGCCTGACATCAAGGA	CGGAGGGTCTTCAGCTTCT

CD, cluster of differentiation; Fw, forward; IFN, interferon; IL, interleukin; ovRPS15, ovine 40S ribosomal protein S15; qPCR, quantitative real-time polymerase chain reaction; Rv, reverse; TNF, tumor necrosis factor.

swine anti-rabbit (1:200) or goat anti-mouse (1:200) from Dako and peroxidase-conjugated goat anti-rabbit (1:200) from Jackson (West Grove, PA, USA) were used. All antibodies were diluted in 0.1% bovine serum albumin in phosphate-buffered saline (PBS).

### Immunohistochemistry

Formalin-fixed terminal ileum was embedded in paraffin and sectioned to 4  $\mu$ m. Inflammatory cells were identified by immunohistochemical staining for T-lymphocytes (CD3), FoxP3, and MPO synthesized mainly by neutrophils. Maturation of fetal intestine was assessed by immunohistochemical staining for I-FABP. Proliferating and apoptotic cells were identified by Ki-67 and caspase-3 staining, respectively. Endogenous peroxidase activity was blocked with either 0.3% H<sub>2</sub>O<sub>2</sub> diluted in TBS (MPO), PBS (CD3, FoxP3, Ki-67, and caspase-3), or methanol (I-FABP). Nonspecific binding was blocked with normal goat serum (MPO, 10%; FoxP3, 20%; and Ki-67, 5%) and bovine serum albumin (CD3, 5% and I-FABP, 5%) for either 30 min (MPO, CD3, and FoxP3) or 1 h (I-FABP and Ki-67) at room temperature and the sections were incubated with the primary antibody as appropriate. After washing, sections were incubated with the selected secondary-conjugated antibody. CD3, FoxP3, Ki-67, and caspase-3 antibodies were recognized with streptavidin-biotin method (DakoCytomation) and antibodies against MPO and I-FABP were recognized with a peroxidase-conjugated secondary antibody. Substrate staining for MPO and I-FABP was performed with 3-amino-9-ethylcarbazole (Sigma); hematoxylin was used as a counterstain for nuclei. Immunoreactivity for CD3, FoxP3, Ki-67, and caspase-3 was detected by using nickel-DAB. Except for I-FABP, the positive stained cells were counted in three high-power fields. The average number of positive cells per high-power field per animal is given. Maturity of the fetal intestine was evaluated based on the size of vacuoles and the localization of I-FABP.

### Immunofluorescence

Tight junction morphology was evaluated by immunofluorescence staining against ZO-1 as described previously.<sup>15</sup> Briefly, ileal cryosections (4  $\mu$ m) were incubated with anti-ZO-1 followed by Texas Red-conjugated goat-anti-rabbit as a secondary antibody and 4',6'-diamino-2-phenyl indole as a stain for the nuclei. The distribution of ZO-1 was examined in  $\times$ 400 magnification using an AxioCam MRc5 camera (Zeiss, Jena, Germany) mounted on an ECLIPSE E800 fluorescence microscope (Nikon, Amsterdam, The Netherlands).

### RNA Isolation and qPCR

Total RNA was extracted from ileum tissue using Trizol Reagent (Invitrogen, Breda, The Netherlands), according to the manufacturer's guidelines. DNA contamination was removed by using RQ1 DNase Kit (Promega, Madison, WI, USA) following the manufacturer's instructions. The digestion of genomic DNA was confirmed by polymerase chain reaction (PCR) using ovine  $\beta$ -actin (forward sequence: 5'-CAGCACAGGCCTCTCGCCTTC-3'; reverse sequence: 5'-CTGGGTCATCTTCTCACGGTTGG-3'). Reverse transcription was performed by using M-MLV Reverse transcriptase (Invitrogen, Bleiswijk, The Netherlands) according to the supplier's recommendations, using oligo-DT primers. Ten nanograms of cDNA was amplified with LightCycler 480 SYBR Green I Master (Roche Applied Science, Almere, The Netherlands). qPCR was performed using the LightCycler 480 (Roche) with primers designed on ovine-specific sequences (Table 2). Melt-curve analysis was performed following completion of qPCR amplifications revealing a single peak for each investigated amplicon, confirming the detection of a specific product. The results were normalized to ovine 40S ribosomal protein S15 (ovRPS15) and mean fold changes in mRNA expression relative to control are presented.

**Statistical Analysis**

Data are presented as mean  $\pm$  s.d. Statistical analysis was performed using GraphPad Prism software (version v.5.0;

GraphPad Software) by using a nonparametric Kruskal–Wallis test followed by Dunn’s *post hoc* test. Differences were considered statistically significant at  $P < 0.05$ .

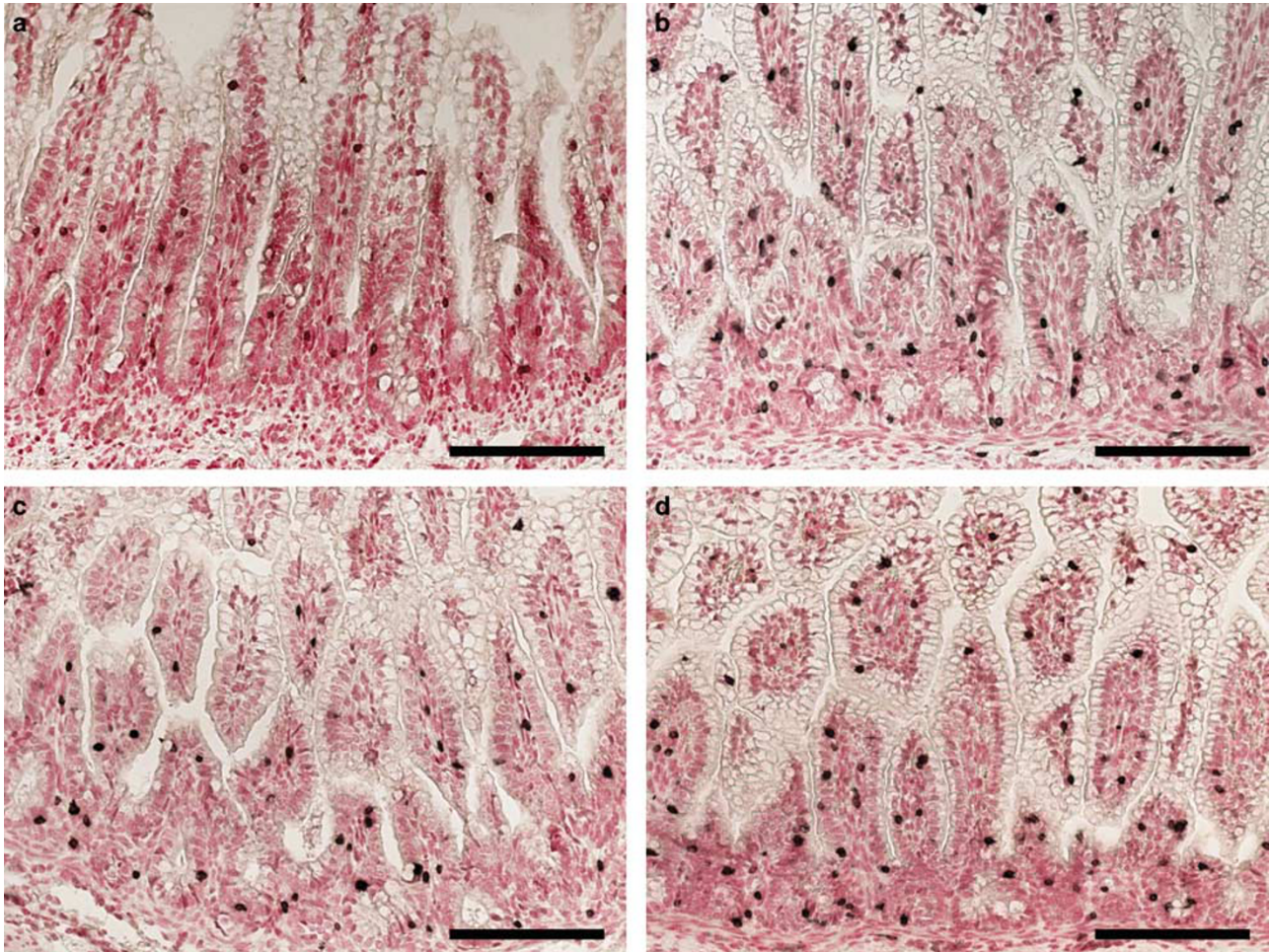


**Figure 1** Number of T-lymphocytes in the fetal intestine. Representative sections of fetal ileum were stained by immunohistochemistry for CD3+ cells of control (a), 6 days interleukin-1 $\alpha$  (IL-1 $\alpha$ ) lung (b), 6 days IL-1 $\alpha$  gut (c), and 6 days IL-1 $\alpha$  snout occlusion (Ocln) (d) animals. For each experimental group, CD3+ expressing cells were counted and the mean cell counts per high-power field per animal is given (e). Scale bar: 100  $\mu$ m. Data are presented as mean  $\pm$  s.d. \* $P < 0.05$ , \*\* $P < 0.01$ , and \*\*\* $P < 0.001$  compared with control. CD3, cluster of differentiation 3; d, day(s); IL-1 $\alpha$ , interleukin-1 $\alpha$ .

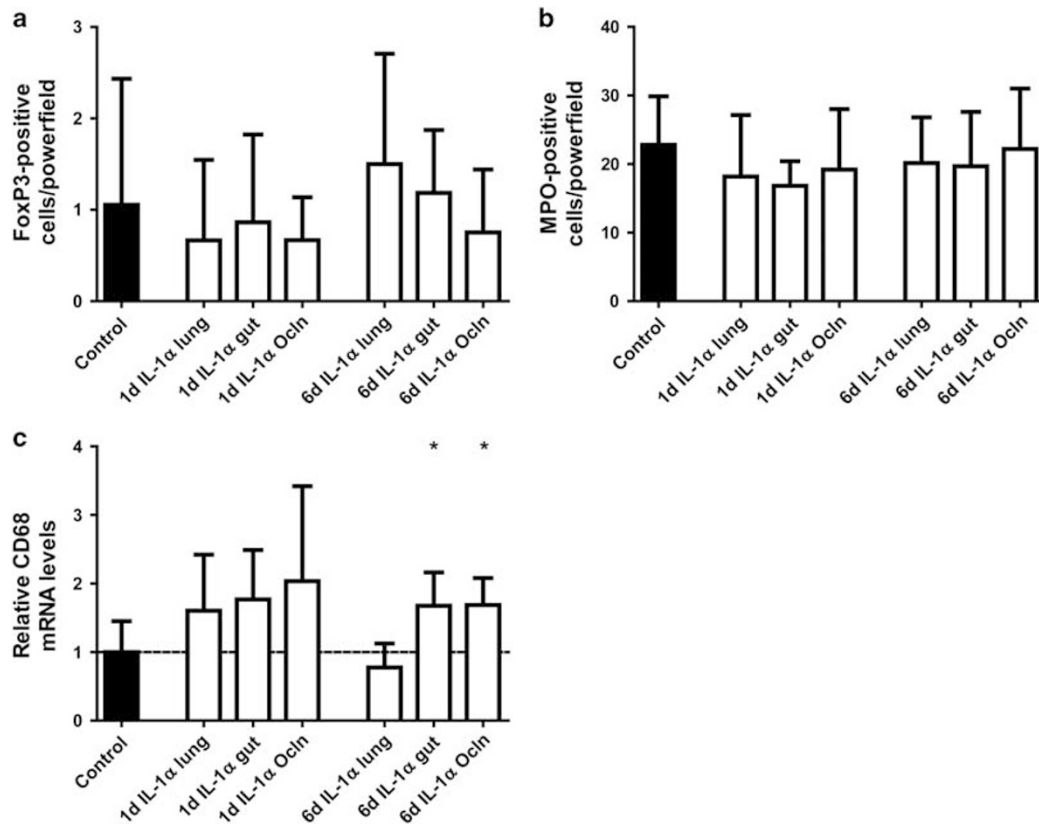


**Figure 2** Number of inflammatory cells in the fetal ileum. For each experimental group, positive expressing cells of FoxP3+ (a) and MPO+ (b) were counted and the mean cell counts per high-power field per animal is given. The mRNA levels of cluster of differentiation 68 (CD68) (c) were evaluated by quantitative real-time polymerase chain reaction (qPCR) and the values were normalized to ovine 40S ribosomal protein S15 (ovRPS15) rRNA levels. Data are presented as mean  $\pm$  s.d. \* $P$  < 0.05 compared with control. d, day(s); FoxP3, forkhead box P3; IL-1 $\alpha$ , interleukin-1 $\alpha$ ; MPO, myeloperoxidase.

## RESULTS

### Inflammatory Cells in the Fetal Ileum After Selective Exposure of Lung, Gut, or Chorioamnion/Skin to IL-1 $\alpha$

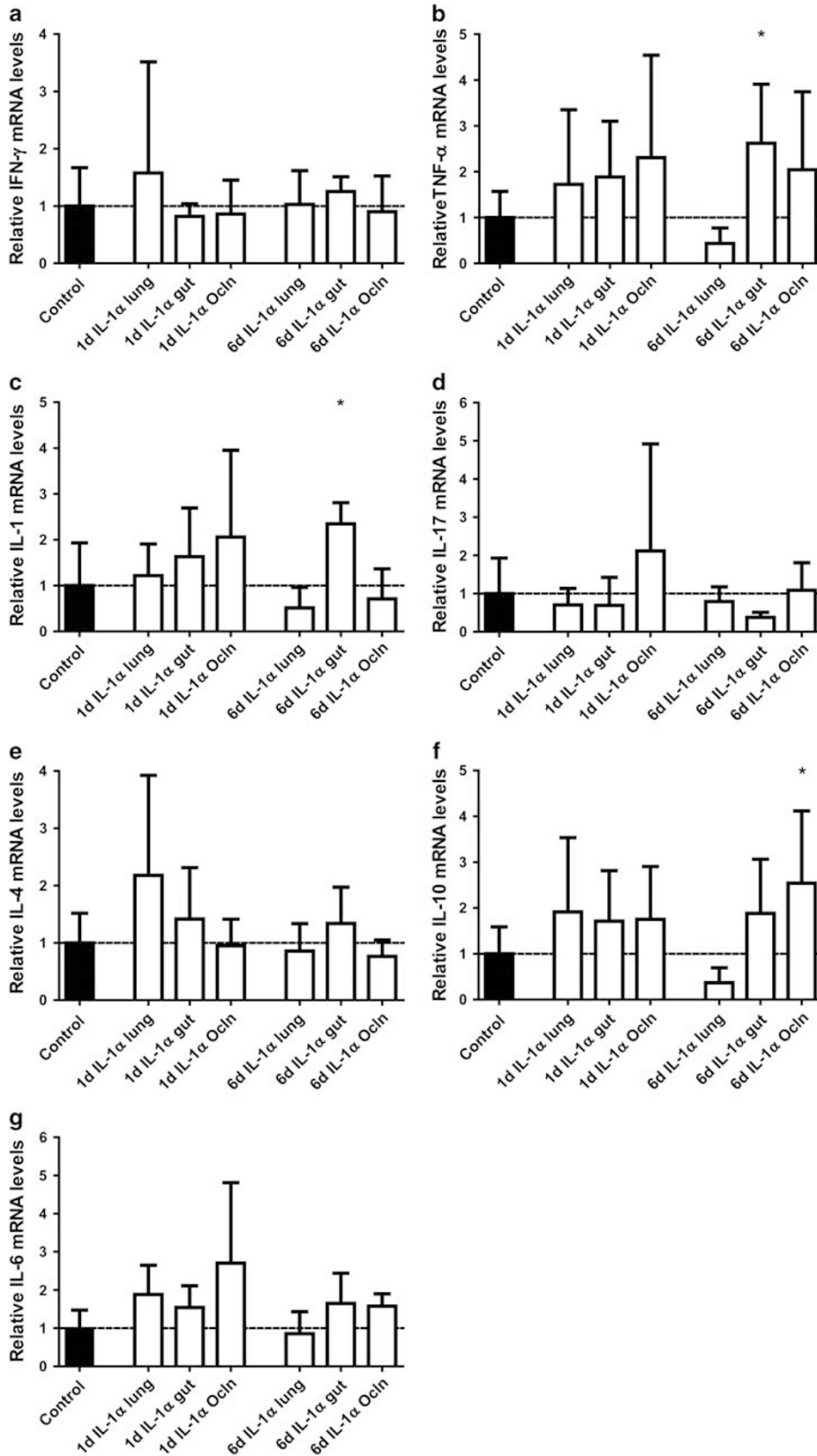
We evaluated the accumulation of inflammatory cells in the gut after IL-1 $\alpha$  exposure to the lung, gut, or chorioamnion/skin by immunohistochemistry. Direct IL-1 $\alpha$  exposure to the gut resulted in increased numbers of CD3+ cells in the fetal ileum when compared with control animals at 1 day after IL-1 $\alpha$  infusion. CD3+ cells in the fetal ileum remained unchanged at 1 day after IL-1 $\alpha$  exposure to the lung or chorioamnion/skin when compared with controls (Figure 1). At 6 days, IL-1 $\alpha$  increased the numbers of CD3+ cells in the fetal ileum in all experimental groups when compared with controls (Figures 1a–e).

In contrast, the number of immunosuppressive regulatory T cells,<sup>26</sup> expressing the transcription factor FoxP3,<sup>27</sup> remained unchanged in the fetal gut at 1 or 6 days after IL-1 $\alpha$  infusion in any fetal compartment when compared with controls (Figure 2a). Similarly, the number of MPO+ cells in the fetal intestine was comparable to control animals after 1 or 6 days of IL-1 $\alpha$  exposure to any fetal compartment (Figure 2b).

Intestinal mRNA levels of CD68, a marker for activated macrophages, were analyzed by qPCR. At 1 day after IL-1 $\alpha$  infusion in all compartments, CD68 mRNA levels remained unaltered in the fetal ileum when compared with controls (Figure 2c). At 6 days, IL-1 $\alpha$  infusion to the lung did not change the mRNA levels of CD68 in the fetal gut compared with controls, whereas the mRNA levels of CD68 were increased when the gut or chorioamnion/skin were exposed to IL-1 $\alpha$  (Figure 2c).

### Cytokine mRNA Levels in the Fetal Gut After IL-1 $\alpha$ Exposure in the Different Fetal Compartments

To further characterize the intestinal inflammatory responses following selective exposure of IL-1 $\alpha$  to the lung, gut, and chorioamnion/skin, mRNA levels of pro- and anti-inflammatory cytokines were evaluated by qPCR. Ileal mRNA levels of IFN- $\gamma$ , TNF- $\alpha$ , IL-1, IL-17, IL-4, IL-10, and IL-6 remained unaltered at 1 day after any of the IL-1 $\alpha$  exposures (Figure 3). Compared with controls, gut mRNA levels of TNF- $\alpha$  and IL-1 were significantly increased at 6 days after IL-1 $\alpha$  exposure to the GI tract (Figures 3b and c), whereas these cytokines remained unaltered when the lung or



chorioamnion/skin were exposed to IL-1 $\alpha$  (Figures 3b and c). The intestinal mRNA levels of IL-10 were increased 6 days after IL-1 $\alpha$  exposure to the chorioamnion/skin (Figure 3f), whereas no differences were observed in the rest of the groups when compared with controls (Figure 3f). The gut mRNA levels of IFN- $\gamma$ , IL-17, IL-4, and IL-6 remained unaltered 6 days after IL-1 $\alpha$  infusion to any fetal compartment (Figures 3a, d, e, and g).

### Gut Injury and Morphological Changes After Selective IL-1 $\alpha$ Exposure to the Gut, Lung, or Chorioamnion/Skin

We first evaluated whether selective IL-1 $\alpha$  exposure to different epithelial surfaces resulted in morphological changes in the fetal intestine by histochemical H&E staining. No clear

signs of intestinal epithelial injury were observed at 1 or 6 days after IL-1 $\alpha$  infusion to any fetal compartment (data not shown). This finding was also confirmed by immunohistochemical analysis of I-FABP, a protein that is expressed by intestinal epithelial cells and is released upon epithelial injury.<sup>28,29</sup>

We then assessed whether selective IL-1 $\alpha$  exposure to different fetal compartments resulted in impaired gut development. Maturation of the fetal gut was assessed by immunohistochemical staining of I-FABP<sup>30</sup> and by the size of vacuoles in the intestinal epithelium. In control animals (Figure 4a), I-FABP expression was detected along the villus, which is characteristic for animals of this GA.<sup>17</sup> In contrast, 6 days after IL-1 $\alpha$  exposure to the gut, I-FABP expression was primarily localized in the crypts (Figure 4b) and large

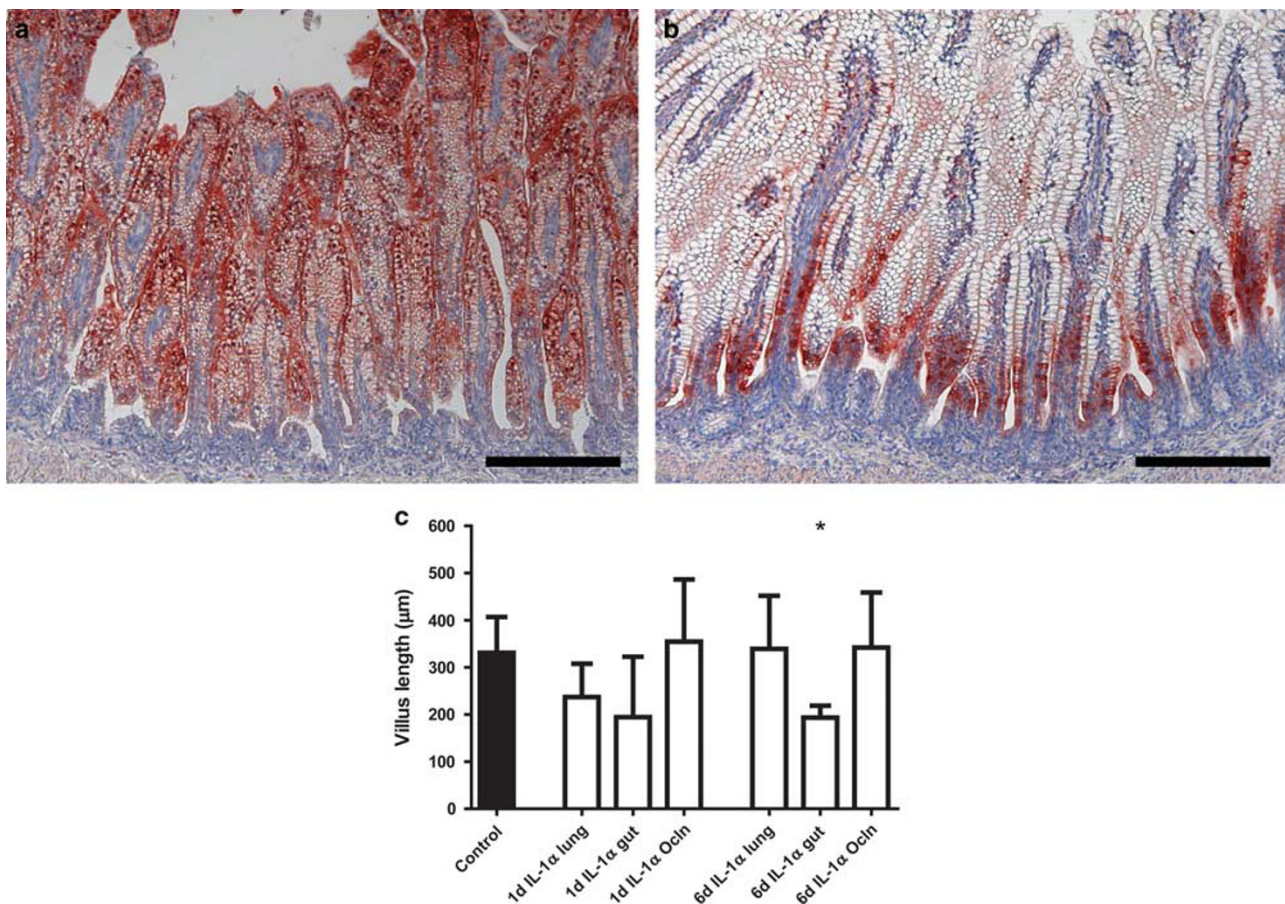


**Figure 4** Maturation of the fetal intestine was evaluated by morphological changes determined by staining for intestinal fatty acid-binding protein (I-FABP). In control animals, the expression of I-FABP was localized across the villi (a). In contrast, interleukin-1 $\alpha$  (IL-1 $\alpha$ ) exposure to the gut resulted in I-FABP expression in the lower villi and revealed enlarged vacuoles along the epithelium at 6 days after infusion (b), a characteristic of immaturity. The villus length was significantly decreased 6 days after direct IL-1 $\alpha$  exposure to the gut compared with controls (c). Scale bar: 200  $\mu$ m. Data are presented as mean  $\pm$  s.d. \* $P$  < 0.05 compared with control. d, day(s).

**Figure 3** Cytokine mRNA levels in fetal ileum of animals exposed to interleukin-1 $\alpha$  (IL-1 $\alpha$ ). The inflammatory cytokines: interferon- $\gamma$  (IFN- $\gamma$ ) (a), tumor necrosis factor- $\alpha$  (TNF- $\alpha$ ) (b), IL-1 (c), IL-17 (d), IL-4 (e), IL-10 (f), and IL-6 (g) were assessed by quantitative real-time polymerase chain reaction (qPCR), and the values for each cytokine were normalized to ovine 40S ribosomal protein S15 (ovRPS15) rRNA levels. Data are presented as mean  $\pm$  s.d. \* $P$  < 0.05 compared with control. d, day(s).

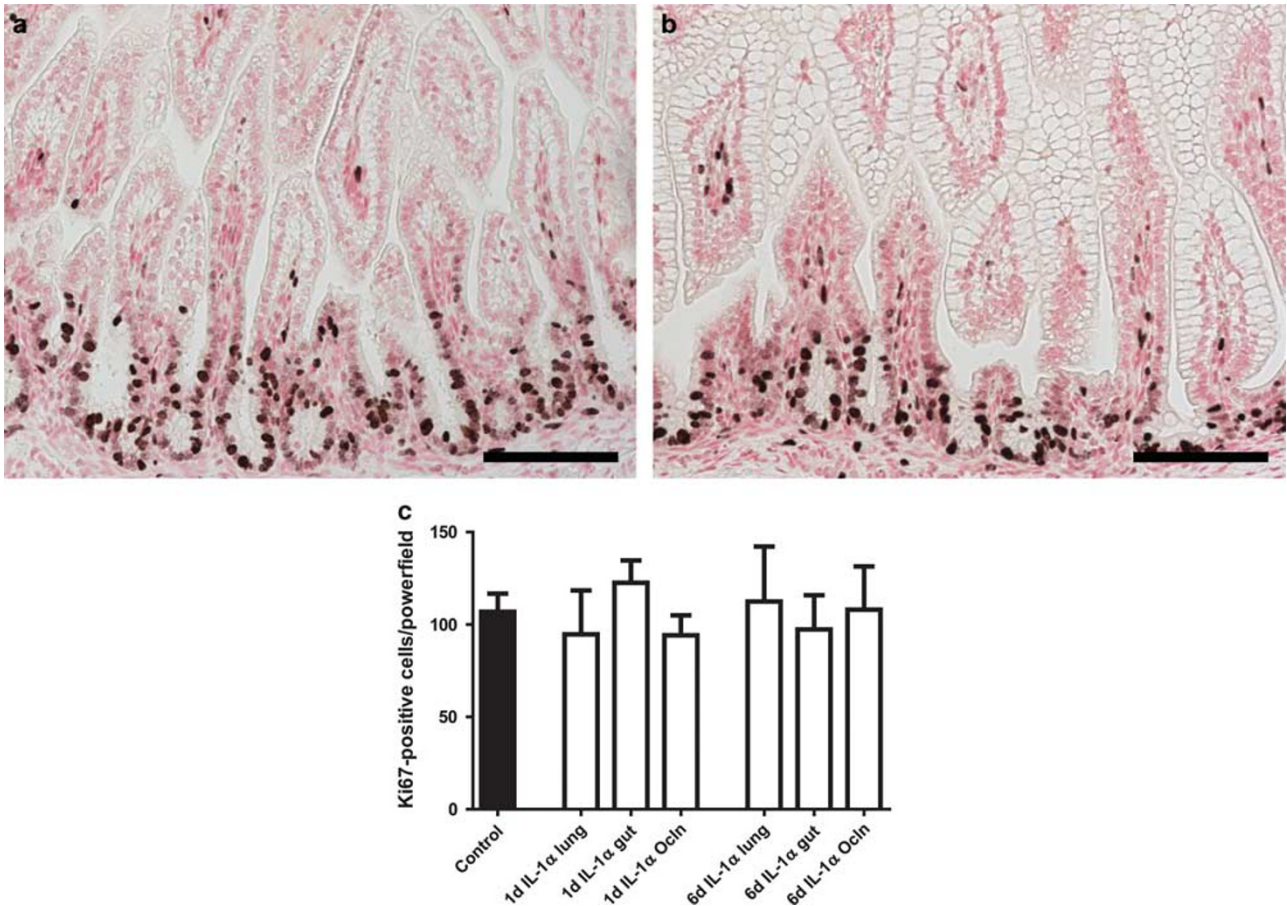


**Figure 5** Distribution of Ki-67-positive cells in the fetal ileum of animals exposed to interleukin-1 $\alpha$  (IL-1 $\alpha$ ). Representative intestinal sections of control (a) and 6 days IL-1 $\alpha$  gut (b) were stained by immunohistochemistry for Ki-67-positive cells. No differences were observed between control and IL-1 $\alpha$  lung-, gut-, and chorioamnion/skin-exposed animals (c). For each experimental group, Ki-67-positive expressing cells were counted and the mean cell counts per high-power field per animal is given (c). Scale bar: 100  $\mu$ m. Data are presented as mean  $\pm$  s.d. d, day(s).

vacuoles were detected in the fetal intestine when compared with controls, indicative of intestinal prematurity (Figure 4b). No significant changes were observed between control and IL-1 $\alpha$  lung- and chorioamnion/skin-exposed animals (data not shown). Finally, direct IL-1 $\alpha$  exposure to the gut resulted in significant shortening of the villus length at 6 days when compared with controls, whereas no changes were observed in villus length 1 or 6 days after IL-1 $\alpha$  exposure to the lung and chorioamnion/skin (Figure 4c).

To gain insight into the mechanism of the observed decreased villus length and the immature intestinal phenotype at 6 days after IL-1 $\alpha$  exposure to the gut, we performed an immunohistochemical staining for the proliferation marker Ki-67 and apoptotic marker caspase-3. No differences were detected in the number of Ki-67- (Figure 5) and caspase-3- (data not shown) positive cells in the intestinal mucosa between control and IL-1 $\alpha$  lung-, gut-, and chorioamnion/skin-exposed animals.

The integrity of tight junctions was evaluated by immunofluorescence staining of ZO-1, an important tight junctional protein in epithelial cells involved in paracellular

permeability.<sup>31</sup> In premature control animals, the distribution of ZO-1 was fragmented (Figure 6a) and this ZO-1 localization in the fetal gut was further disturbed after selective intestinal IL-1 $\alpha$  exposure (Figures 6c and f) with more severe fragmentation at 1 day after IL-1 $\alpha$  infusion to the GI tract (Figure 6c). The ZO-1 distribution pattern in the rest investigated groups was similar to control animals (Figure 6).

**Systemic Immune Activation Following IL-1 $\alpha$  Exposure to the Lung, Gut, or Chorioamnion/Skin**

We examined whether 6 days after selective IL-1 $\alpha$  exposure to the lung, gut, or chorioamnion/skin resulted in systemic inflammation. The number of white blood cells, monocytes, lymphocytes, and neutrophils was increased in cord blood after 6 days of IL-1 $\alpha$  exposure to the lung (Figure 7). Increased number of white blood cells, monocytes, and neutrophils was also observed in cord blood 6 days after IL-1 $\alpha$  exposure to the chorioamnion/skin, whereas the number of lymphocytes was similar to control animals (Figure 7c). The cell counts of white blood cells, monocytes, lymphocytes, and neutrophils in cord blood after 6 days of



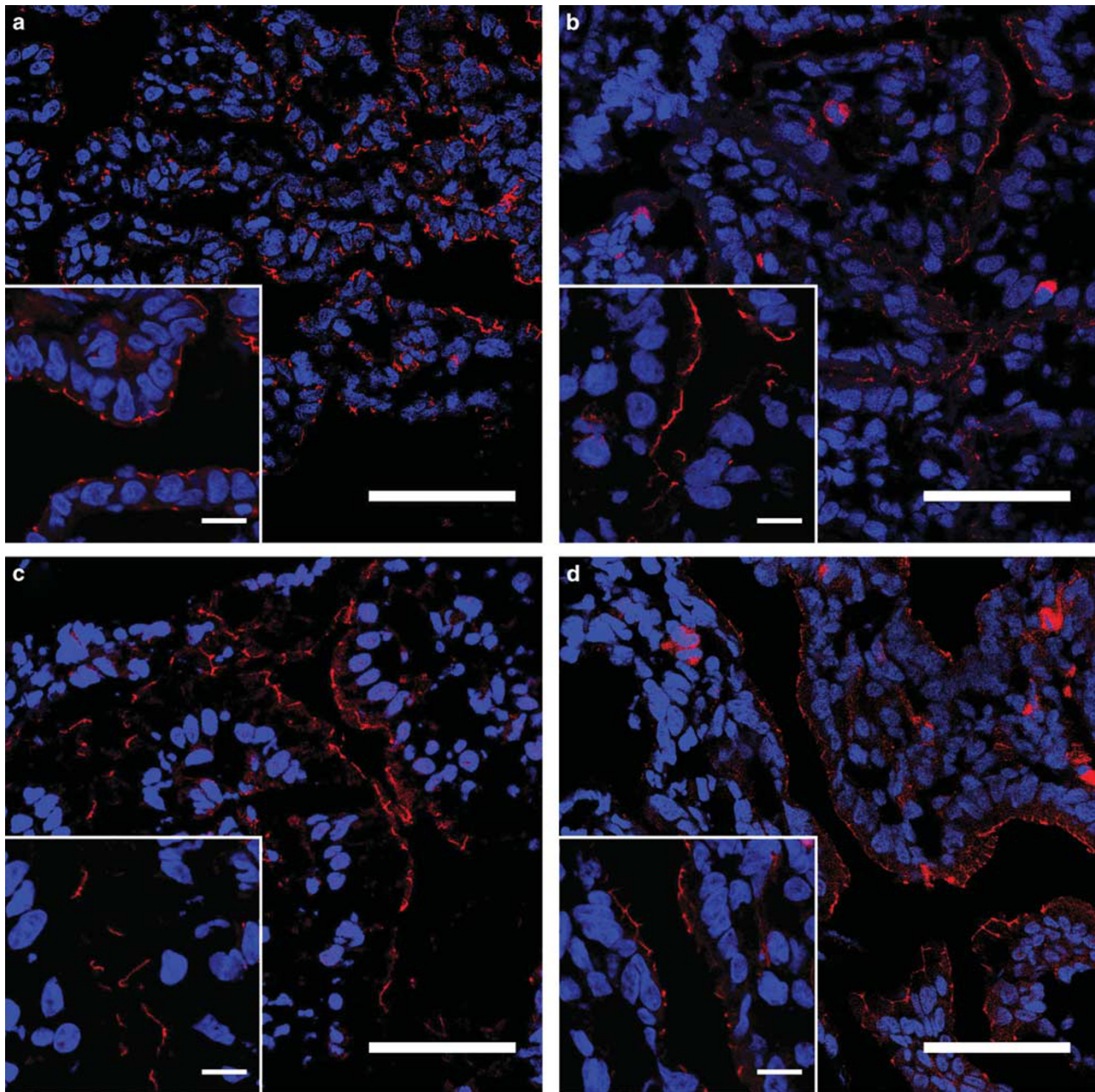


**Figure 6** Distribution of zonula occludens protein-1 (ZO-1) in the fetal ileum of animals exposed to IL-1 $\alpha$ . Control animals had a moderate fragmentation of ZO-1 expression along the epithelium (a). This fragmentation was further disturbed after selective interleukin-1 $\alpha$  (IL-1 $\alpha$ ) exposure to the gut (c and f) with more severe ZO-1 fragmentation at 1 day after IL-1 $\alpha$  infusion to the gastrointestinal (GI) tract (c). The distribution of ZO-1 in (b) 1 day IL-1 $\alpha$  lung, (d) 1 day IL-1 $\alpha$  snout occlusion (Ocln), (e) 6 days IL-1 $\alpha$  lung, and (g) 6 days IL-1 $\alpha$  Ocln animals was similar to the control (a). Scale bar: 50  $\mu$ m. Scale bar in insets: 10  $\mu$ m.

IL-1 $\alpha$  exposure to the gut were not different when compared with controls.

## DISCUSSION

We previously demonstrated that inhibition of IL-1 signaling in the course of ureaplasma-induced chorioamnionitis substantially prevented inflammation, disturbed maturation, and injury of the fetal intestine.<sup>17</sup> In the present study, we

evaluated the impact of IL-1 $\alpha$  signaling on intestinal inflammation and injury when different epithelial organs were selectively exposed to IL-1 $\alpha$ . Our findings indicate that the adverse outcomes of the fetal gut in the course of chorioamnionitis are the combined result of selective IL-1 $\alpha$ -driven signaling of the lung, gut, and chorioamnion/skin. Interestingly, intestinal inflammatory responses were distinct following different sites of IL-1 $\alpha$  exposure and gut injury and

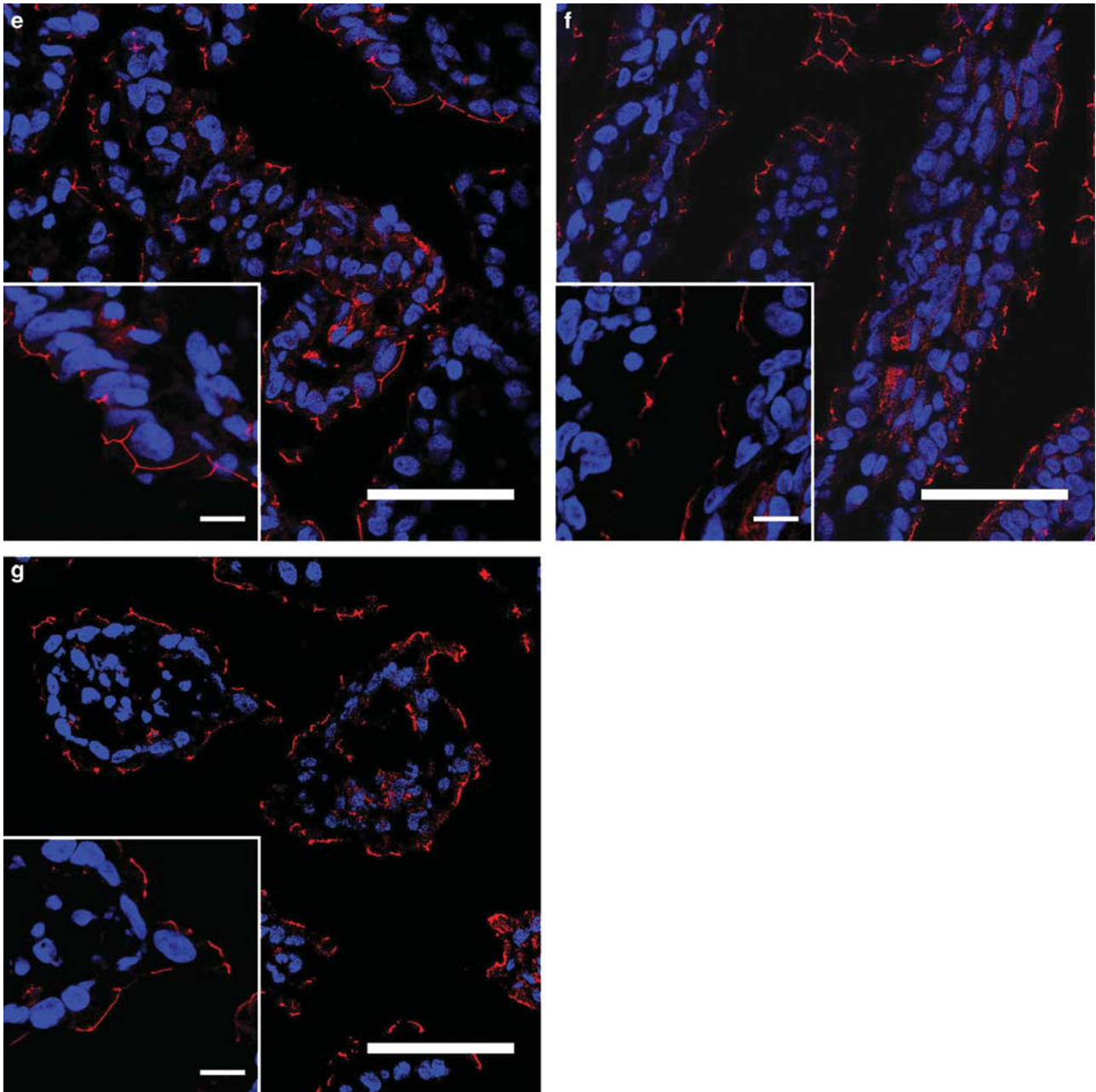


Figure 6 Continued.

immaturity were only induced upon direct contact of IL-1 $\alpha$  to the gastrointestinal mucosa.

At day 1 after IL-1 $\alpha$  infusion into the GI tract, intestinal inflammation was characterized by infiltration of T cells and subsequent tight junctional loss. The current findings confirm and explain our earlier observations, showing that local exposure of the intestinal epithelium to LPS induces lymphocyte influx and impaired gut integrity.<sup>15</sup> In line with these data, *in vitro* experiments with intestinal epithelial cells have shown that IL-1 supplementation in the culture system increased the permeability of tight junctions.<sup>32,33</sup> These

findings indicate that increased intestinal IL-1 $\alpha$  levels directly interact with the intestinal epithelial cells and/or resident immune cells to induce adverse intestinal outcomes as seen in the fetal intestine in the course of chorioamnionitis.

At 6 days, intestinal inflammation appears to be dependent on the route of IL-1 $\alpha$  exposure. In particular, 6 days after direct IL-1 $\alpha$  to the GI tract, intestinal immune activation was characterized by increased TNF- $\alpha$  and IL-1 mRNA levels and moderate signs of tight junctional loss. These current findings provide a mechanistic explanation for previous findings showing that direct gut exposure to LPS induced the

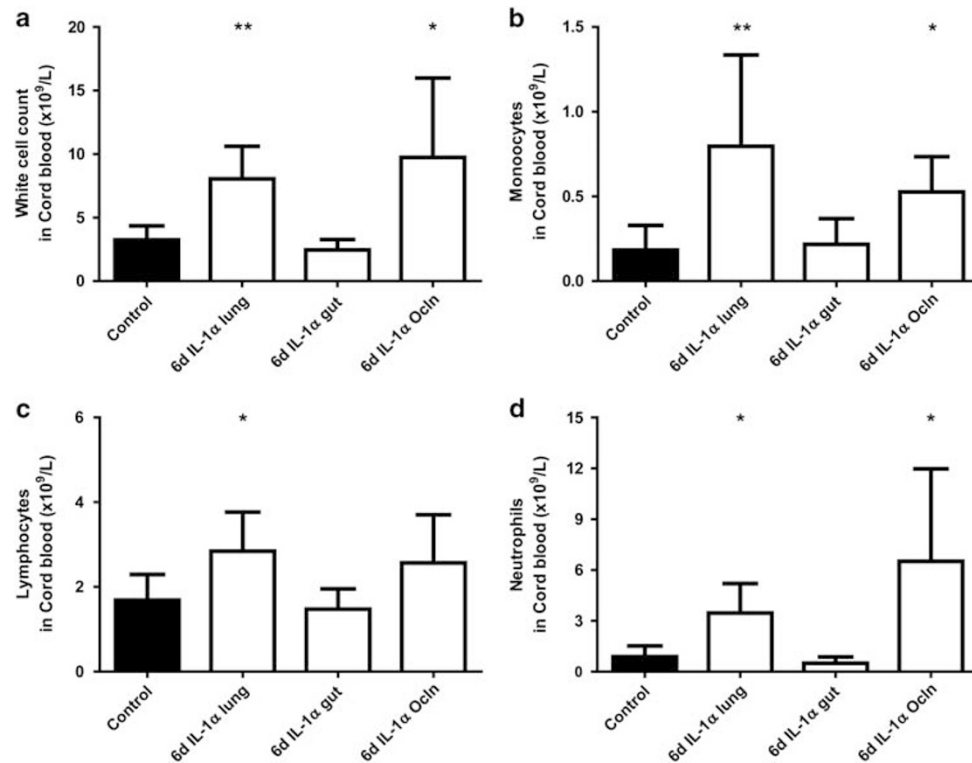


**Figure 7** Differential cord blood counts of white blood cells (a), monocytes (b), lymphocytes (c), and neutrophils (d). Data are presented as mean  $\pm$  s.d. \* $P$ <0.05 and \*\* $P$ <0.01 compared with control. d, day(s); IL-1 $\alpha$ , interleukin-1 $\alpha$ .

expression of these proinflammatory cytokines in the fetal ileum and this increase was associated with intestinal injury.<sup>15</sup>

Intestinal inflammation was associated with an immature intestinal phenotype 6 days after IL-1 $\alpha$  exposure to the GI tract as the villi were shortened, formed by enterocytes with enlarged vacuoles, and I-FABP expression was restricted to the basis of the villi, a characteristic pattern found in the extreme premature gut.<sup>30</sup> Interestingly, these morphological changes were not associated with altered number of Ki-67- or caspase-3-positive cells in the intestinal mucosa at 6 days after IL-1 $\alpha$  exposure to the fetal gut. Therefore, diminished differentiation, rather than altered cell proliferation and/or cell death, appears to be responsible for the observed immature intestinal phenotype at 6 days after IL-1 $\alpha$  exposure to the gut. Development of the fetal intestine was shown to be impaired in an IL-1-dependent manner in the context of chorioamnionitis.<sup>17</sup> Therefore, these results indicate that disturbed maturation of the intestinal epithelium during antenatal inflammation is the result of direct IL-1 $\alpha$  effects to the GI mucosa. Alternatively, increased vacuolization and shortened villi at 6 days after IL-1 $\alpha$  exposure to the fetal gut could also be interpreted as indicators of mucosal injury. However, at this stage increased vacuolization and villus atrophy were not associated with increased apoptosis, shedding of epithelial cells and accumulation of cellular debris in the lumen. Therefore, the shortening of the villi might originate from inflammation-induced smooth muscle reactivity and/or inflammation-driven

changes of the subepithelial architecture of myofibroblasts within the villus compartment.<sup>34</sup>

Systemic inflammation was associated with intestinal inflammation 6 days after IL-1 $\alpha$  exposure to the chorioamnion/skin. This finding is in contrast with previous reports demonstrating that LPS exposure to the chorioamnion/skin provoked a systemic response without inducing intestinal immune activation.<sup>15,35</sup> This discrepancy could be explained by the relative low number of circulating monocytes when compared with LPS<sup>35</sup> after IL-1 $\alpha$  infusion into the snout occluded animals, which was paralleled by increased CD68 (macrophages) mRNA levels in the fetal gut, indicating influx and/or differentiation of monocytes from the periphery. It is tempting to speculate that intestinal macrophages in the GI tract following IL-1 $\alpha$  exposure to the chorioamnion/skin might be responsible for the accumulation of T cells in the fetal gut.<sup>36</sup> This intestinal immune response at 6 days after IL-1 $\alpha$  administration to the chorioamnion/skin appeared to have an anti-inflammatory character as upregulated mRNA levels of IL-10, a cytokine that has central role in maintaining gut wall integrity,<sup>37,38</sup> were detected and associated with the absence of epithelial damage in the fetal ileum.

The intestinal immune response 6 days after IL-1 $\alpha$  intratracheal infusion was characterized by marginal inflammatory changes in the fetal gut with no signs of mucosal injury. In contrast, we have shown that intratracheal LPS delivery results in intestinal inflammation and mucosal

damage.<sup>15</sup> These findings imply that induction of intestinal epithelial damage after pulmonary-mediated (systemic) immune activation are largely IL-1-independent.

Although the mechanisms by which the fetal intestine responds to indirect IL-1 $\alpha$  exposure to the lung or chorioamnion/skin remain to be elucidated, the current study provides evidence that direct IL-1 $\alpha$  exposure to these epithelial organs (i.e. lung and chorioamnion/skin) can trigger gut inflammatory processes in the course of chorioamnionitis. Since not only the gut but also the lung and chorioamnion/skin seem to have a role in IL-1 $\alpha$ -mediated inflammatory changes of the fetal gut during chorioamnionitis, future therapeutic interventions may need to focus on targeting both IL-1 $\alpha$  local and systemically mediated immune responses during antenatal inflammation.

In conclusion, we have shown that IL-1 $\alpha$  signaling in different fetal compartments contributes to the induction of intestinal inflammation in the course of chorioamnionitis. Importantly, altered gut development and mucosal injury required direct contact of IL-1 $\alpha$  to GI epithelium, which emphasized the crucial role of local IL-1 $\alpha$ -driven intestinal inflammatory processes in the context of chorioamnionitis.

#### ACKNOWLEDGMENTS

We thank Nico Kloosterboer and Lilian Kessels for the excellent technical support.

#### DISCLOSURE/CONFLICT OF INTEREST

The authors declare no conflict of interest.

1. Goldenberg RL, Culhane JF, Iams JD *et al*. Epidemiology and causes of preterm birth. *Lancet* 2008;371:75–84.
2. Kemp MW. Preterm birth, intrauterine infection, and fetal inflammation. *Front Immunol* 2014;5:574.
3. Ericson JE, Laughon MM. Chorioamnionitis: implications for the neonate. *Clin Perinatol* 2015;42:155–165.
4. Galinsky R, Polglase GR, Hooper SB *et al*. The consequences of chorioamnionitis: preterm birth and effects on development. *J Pregnancy* 2013;2013:412831.
5. Romero R, Miranda J, Kusanovic JP *et al*. Clinical chorioamnionitis at term I: microbiology of the amniotic cavity using cultivation and molecular techniques. *J Perinat Med* 2015;43:19–36.
6. Gantert M, Been JV, Gavilanes AW *et al*. Chorioamnionitis: a multiorgan disease of the fetus? *J Perinatol* 2010;30:521–530.
7. Kallapur SG, Presicce P, Rueda CM *et al*. Fetal immune response to chorioamnionitis. *Semin Reprod Med* 2014;32:56–67.
8. Denzler A, Burkhardt T, Natalucci G *et al*. Latency after preterm prelabor rupture of the membranes: increased risk for periventricular leukomalacia. *J Pregnancy* 2014;2014:874984.
9. Paul DA, Zook K, Mackley A *et al*. Reduced mortality and increased BPD with histological chorioamnionitis and leukocytosis in very-low-birth-weight infants. *J Perinatol* 2010;30:58–62.
10. Been JV, Lievens S, Zimmermann LJ *et al*. Chorioamnionitis as a risk factor for necrotizing enterocolitis: a systematic review and meta-analysis. *J Pediatr* 2013;162:236–242; e232.
11. Coggins SA, Wynn JL, Weitkamp JH. Infectious causes of necrotizing enterocolitis. *Clin Perinatol* 2015;42:133–154.
12. Kallapur SG, Willet KE, Jobe AH *et al*. Intra-amniotic endotoxin: chorioamnionitis precedes lung maturation in preterm lambs. *Am J Physiol Lung Cell Mol Physiol* 2001;280:L527–536.
13. Kramer BW, Moss TJ, Willet KE *et al*. Dose and time response after intraamniotic endotoxin in preterm lambs. *Am J Respir Crit Care Med* 2001;164:982–988.
14. Zhang L, Saito M, Jobe A *et al*. Intra-amniotic administration of *E coli* lipopolysaccharides causes sustained inflammation of the fetal skin in sheep. *Reprod Sci* 2012;19:1181–1189.
15. Wolfs TG, Kramer BW, Thuijls G *et al*. Chorioamnionitis-induced fetal gut injury is mediated by direct gut exposure of inflammatory mediators or by lung inflammation. *Am J Physiol Gastrointest Liver Physiol* 2014;306:G382–G393.
16. Kallapur SG, Nitsos I, Moss TJ *et al*. IL-1 mediates pulmonary and systemic inflammatory responses to chorioamnionitis induced by lipopolysaccharide. *Am J Respir Crit Care Med* 2009;179:955–961.
17. Wolfs TG, Kallapur SG, Knox CL *et al*. Antenatal ureaplasma infection impairs development of the fetal ovine gut in an IL-1-dependent manner. *Mucosal Immunol* 2013;6:547–556.
18. Vadillo-Ortega F, Sadowsky DW, Haluska GJ *et al*. Identification of matrix metalloproteinase-9 in amniotic fluid and amniochorion in spontaneous labor and after experimental intrauterine infection or interleukin-1 beta infusion in pregnant rhesus monkeys. *Am J Obstet Gynecol* 2002;186:128–138.
19. Bry K, Lappalainen U, Hallman M. Intraamniotic interleukin-1 accelerates surfactant protein synthesis in fetal rabbits and improves lung stability after premature birth. *J Clin Invest* 1997;99:2992–2999.
20. Adams Waldorf KM, Rubens CE, Gravett MG. Use of nonhuman primate models to investigate mechanisms of infection-associated preterm birth. *BJOG* 2011;118:136–144.
21. Wolfs TG, Kallapur SG, Polglase GR *et al*. IL-1 $\alpha$  mediated chorioamnionitis induces depletion of FoxP3+ cells and ileal inflammation in the ovine fetal gut. *PLoS One* 2011;6:e18355.
22. Kallapur SG, Kramer BW, Nitsos I *et al*. Pulmonary and systemic inflammatory responses to intra-amniotic IL-1 $\alpha$  in fetal sheep. *Am J Physiol Lung Cell Mol Physiol* 2011;301:L285–L295.
23. Berry CA, Nitsos I, Hillman NH *et al*. Interleukin-1 in lipopolysaccharide induced chorioamnionitis in the fetal sheep. *Reprod Sci* 2011;18:1092–1102.
24. Sosenko IR, Kallapur SG, Nitsos I *et al*. IL-1 alpha causes lung inflammation and maturation by direct effects on preterm fetal lamb lungs. *Pediatr Res* 2006;60:294–298.
25. Nijland MJ, Day L, Ross MG. Ovine fetal swallowing: expression of preterm neurobehavioral rhythms. *J Matern Fetal Med* 2001;10:251–257.
26. Renz H, Brandtzaeg P, Hornef M. The impact of perinatal immune development on mucosal homeostasis and chronic inflammation. *Nat Rev Immunol* 2012;12:9–23.
27. Rocchi MS, Wattedegera SR, Frew D *et al*. Identification of CD4+CD25 high Foxp3+ T cells in ovine peripheral blood. *Vet Immunol Immunopathol* 2011;144:172–177.
28. Grootjans J, Thuijls G, Verdum F *et al*. Non-invasive assessment of barrier integrity and function of the human gut. *World J Gastrointest Surg* 2010;2:61–69.
29. Khadaroo RG, Fortis S, Salim SY *et al*. I-FABP as biomarker for the early diagnosis of acute mesenteric ischemia and resultant lung injury. *PLoS One* 2014;9:e115242.
30. Reisinger KW, Elst M, Derikx JP *et al*. Intestinal fatty acid-binding protein: a possible marker for gut maturation. *Pediatr Res* 2014;76:261–268.
31. Gumber S, Nusrat A, Villingier F. Immunohistological characterization of intercellular junction proteins in rhesus macaque intestine. *Exp Toxicol Pathol* 2014;66:437–444.
32. Capaldo CT, Nusrat A. Cytokine regulation of tight junctions. *Biochim Biophys Acta* 2009;1788:864–871.
33. Lie PP, Cheng CY, Mruk DD. The biology of interleukin-1: emerging concepts in the regulation of the actin cytoskeleton and cell junction dynamics. *Cell Mol Life Sci* 2012;69:487–500.
34. Boshuizen JA, Reimerink JH, Korteland-van Male AM *et al*. Changes in small intestinal homeostasis, morphology, and gene expression during rotavirus infection of infant mice. *J Virol* 2003;77:13005–13016.
35. Kemp MW, Kannan PS, Saito M *et al*. Selective exposure of the fetal lung and skin/amnion (but not gastro-intestinal tract) to LPS elicits acute systemic inflammation in fetal sheep. *PLoS One* 2013;8:e63355.
36. Pabst O, Bernhardt G. The puzzle of intestinal lamina propria dendritic cells and macrophages. *Eur J Immunol* 2010;40:2107–2111.
37. Emami CN, Chokshi N, Wang J *et al*. Role of interleukin-10 in the pathogenesis of necrotizing enterocolitis. *Am J Surg* 2012;203:428–435.
38. Olszak T, Neves JF, Dowds CM *et al*. Protective mucosal immunity mediated by epithelial CD1d and IL-10. *Nature* 2014;509:497–502.